Arab Gulf J. scient. Res. **4** (2), pp. 511-527 (1986)

Genesis of Iron Oxides and Ferruginous Oolites in the Coniacian - Santonian Sequence of the Abu Zenima Area, Sinai, Egypt

El Sayed A.A. Youssef

Faculty of Science, University of Cario, Egypt

ABSTRACT. The pyritic, glauconitic and dolomitic facies within the Coniacian - Santonian sequence of the Abu Zenima area, west-central Sinai, Egypt, display characteristic post-depositional, chemical, mineralogical and textural changes. These changes are mostly attributed to bacterial activity and weathering. The studied microfacies are represented by thin layers of ferruginous pyrite-biomicrite, ferruginous glauconitic oolite, mottled dolostone, and ferruginous glauconitic quartzarenite. The ferruginous ooids are generated in place from the weathering of glauconite grains, whereas the mottled character of the dolostone is produced by the oxidation of ferrous iron released from ankerite and glauconite grains by weathering. The ferruginous materials are composed mainly of hematite, goethite and lepidocrocite.

This study aims to throw light on the genesis of the iron oxides and ferruginous oolites in pyritic, glauconitic, and dolomitic carbonates and in glauconitic quartzarenite facies in the Coniacian - Santonian successions of the Abu Zenima area (Fig. 1). In order to clarify this aim, diagenetic models as well as the effects of weathering are discussed. This discussion is based on field, petrographical, mineralogical and some geochemical studies.

The Coniacian - Santonian sequence in west-central Sinai was first named as the Matulla Formation (type succession in Wadi Matulla) by Ghorab (1961). He described it as a unit composed of about 170 m of interbedded sandstone, shale and marl of Coniacian - Santonian age underlying the Sudr Formation (Campanian - Maestrichtian) and overlying the Wata Formation (Turonian) in conformable relationship. A stratigraphic section with the main microfacies types of this sequence at Abu Zenima area is presented in this work (Fig. 2). The terms employed in the microfacies description follow those proposed by Folk (1974).

Mineralogical and geochemical investigations were performed using X-ray diffraction, a Jeol Scanning Electron microscope (S.E.M.) JSM-35 with Kevex Mx 7000 system and a Unicam Sp 90A series 2 atomic absorption spectrophotometer.

Microfacies Types

Petrographic study reveals that the iron oxides in the Coniacian - Santonian sediments occur in the following microfacies types:

1. *Ferruginous Pyrite - Biomicrite*

The thickness of ferruginous pyrite - biomicrite layer is about 40 cm. It overlies and gradually changes into about 30 cm of yellowish brown dolomitic biomicrite. This microfacies is made up mainly of tiny framboids of oxidised crystals which form about 80% of the framework, and about 20% obliterated shell fragments and benthonic forams. The framework is cemented with ferruginous micrite which is extensively aggraded into sparry calcite. Pore spaces and fractures are mostly filled with gypsum and sparry calcite. Thin (~mm) argillaceous layers are sometimes intercalated with the biomicrite. Studies by the SEM show that the framboidal texture is formed of aggregates of anhedral crystals (Fig. 3A). These crystals are composed of iron and sulphur as shown by the distribution pattern of these elements (Fig. 3 B and C). The oxidised iron sulphide crystals disseminated in the sparry calcite generally exhibit clear sharp boundaries, whereas those in the micrite and argillaceous layers have a surrounding oxide halo and lack clear boundaries.

2. *Ferruginous Glauconitic Oolites*

This microfacies occurs at the base of a transgressive phase (Fig. 2). It attains a thickness of about 60 cm and is generally composed of greenish yellow to yellowish brown ooids forming about 60% of the total grains, 20% yellowish green glauconite grains, 15% quartz grains and about 5% ostracods and molluscan shell fragments. The grains are generally embedded in a ferruginous argillaceous matrix. However, fractures and pore spaces are filled with sparry calcite and silica. Thin (~mm) sandy ferruginous argillaceous layers are generally intercalated in this microfacies.

The ooids are mostly rounded, elliptical and some of them are irregular and semi-circular in form. They consist of either greenish yellow nuclei surrounded by concentric layers or concentric layers without nuclei. The concentric layers range in colour from red to orange. Some grains have more than one nucleus defining a composite ooid form. The boundary between nuclei and layers are generally gradational. The glauconite grains are also rounded elliptical and generally fissured especially at the boundaries. Some glauconite grains have one red marginal layer showing superficial ooid development. SEM studies show that the nuclei and the

concentric layers generally exhibit the same features and characters (Fig. 3D and 4A). This may indicate that they have the same genesis. They are formed mainly of iron (Fig. 4B) with traces of silica (Fig. 4C) and alumina whereas calcium occur mainly in fractures inside the ooids (Fig. 4D). These petrographic characteristics and microchemical analysis shown by the distribution patterns of iron, silica and calcium may suggest that the original grains were of glauconitic composition. Both glauconite and ooid grains show well-defined boundaries and exhibit transitional stages (Fig. 5A, i-iv). Quartz grains are fine to medium, moderately sorted, subangular and mostly with authigenic overgrowths. The overgrowths are in perfect optical continuity and are separated from the original grains by a line of impurities. Some quartz grains are etched by corrosion vugs at their boundaries (Fig. 4C).

The ferruginous glauconitic oolite facies is overlain by about 1.5 m of ostracod - pelbiosparite and mottled dolostone. The ostracod - pelbiosparite is composed of rounded and elliptical calcareous grains with diameters ranging between 0.2 to 0.8 mm forming more than 60% of the grains, 30% ostracods and molluscan shell fragements and about 10% fine, subangular, well sorted quartz grains. The grains are cemented with microsparite which is mostly aggraded into sparry calcite. The rounded and elliptical calcareous grains are interpreted as algal pellets and grains (Wolf 1965), referred as pseudo-oncoids by Dahanayake (1977).

3. *Mottled Dolostone*

The mottled dolostone microfacies is composed of hypidiotopic to idiotopic sucrosic dolostone (Folk 1973). The dolomite crystals have an average diameter of about 60 μm and are of ankeritic composition. Ankerite crystals are characterised by successive alternations of clear and ferruginous zones which are generally alligned parallel to cleavage planes. However, the majority have clear center and ferruginous boundaries. Some of the crystals are hematite pseudomorphs after rhombic ankerite. Other ankerite crystals have been replaced by granular calcite, indicating a recalcification (dedolomitization) process. The mottled character is due to elongate, rounded, dark brown patches scattered in a yellowish brown groundmass of ankerite. They are generally irregularly distributed and with a maximum size of about 2 cm and have sharp boundaries. Figures (5B, i-iv) show the petrographic evolution of the mottled dolostone.

4. *Ferruginous Glauconitic Quartzarenite*

This facies is generally intercalated with sandy algal oobiopelsparite facies at the top part of the Coniacian - Santonian sequence in the study area. They have a variable thickness (from 2-15 m thick) and represent the base of the second transgressive phase (Fig. 2). The colour of this facies varies graditionally from yellowish green, greenish yellow, reddish brown to black, depending upon

intensity of weathering. It consists of medium size, well-sorted, subangular quartz grains forming about 75% of the grains, 20% glauconite grains and about 5% feldspar. In the greenish yellow facies the framework is cemented with either silica overgrowths or ankerite and sparry calcite whereas in the reddish brown and black facies the cement is mainly ferruginous material. The silica overgrowths are generally separated from the original quartz grains by a line of impurities and are in optical continuity. Some of the quartz grains are corroded by the growing ankerite rhombs, whereas the majority of them are extensively etched and divided into several pieces by the ferruginous material (Fig. 5C, i-iv) indicating an *in situ* incongruent dissolution. The glauconite grains are represented by rounded, irregular grains and film facies (Odin 1975). The glauconite films generally encrust the quartz grains, but they are interpreted as having been deposited in intergranular pores (Odin, *op. cit.*).

Diagenetic Models

Formation of Framboidal Pyrite

The genesis of low temperature pyrite and the role of sulphate reducing bacteria in its formation have been studied experimentally and in Recent sediments by many authors (review by Goldhaber and Kaplan 1974; Krouse and McCreaday 1979).

Goldhaber and Kaplan (1974) and Sweeney and Kaplan (1973) concluded that pyrite does not normally form by direct precipitation but is preceded by fine grained and poorly crystallised metastable mackinawite and greigite. However, the direct formation of pyrite from solution has recently been reported by Howarth (1979) in salt marshes and Clark and Lutz (1980) in shells of living bivalves.

The geochemical analysis of many polished thin sections by the SEM shows that the oxidised crystals which form about 80% of the framework were originally iron sulphide. However, the mineralogical studies by X-ray diffraction do not show a pyrite pattern in most of these samples, but in a few samples a weak pyrite pattern is recognized. This may indicate that most of these iron sulphides are represented by poorly crystalline phases, which suggesting the mode of formation of pyrite proposed by Goldhaber and Kaplan (1974) and Sweeney and Kaplan (1973).

The studied iron sulphides are believed to have formed through the activity of sulphate reducing bacteria during diagensis at the time of burial. The source of sulphur was from the saline water in the pore spaces and the organic matter of the buried organisms. More than one source of iron essential for pyrite formation is suggested. It could be supplied as transported particles of iron oxide or absorbed on clays in the ferric state. Iron in clay mineral lattice may also be an important

source (Siever and Kastner 1972, Grossman *et al.* 1979). Another important source of iron (believed to be the main agency for pyrite formation in the studied microfacies) is the ferruginous micrite matrix which is now aggraded into sparite cement.

The observation that the pyrite-biomicrite is overlain and gradually passes into dolomitic biomicrite suggests that under favourable reducing condition just below the redox boundary in the lower part of the sediments, ferric iron and sulphate were reduced to ferrous iron and H_2S and then to HS^- respectively by the reducing bacteria. Both Fe^{2+} and HS^- combined to form iron sulphides. However, under slight oxidising conditions in the upper part of the sediments, the organic matter was oxidised, mostly by aerobic bacteria, giving CO_3^{2-}. In the presence of some nuclei (microcrystalline dolomite crystal, Morrow 1982), the produced CO_3^{2-} combined with Mg^{2+} and iron from the pore water and the ferruginous micrite to form ankerite. This type of dolomite is similar to the euhedral micrometer size dolomite rhombs that are scattered in the Recent sediments forming Andros Island (Gebelein *et al.* 1980) and may record the beginning of a progression towards a totally dolomitized fabric (sucrosic dolostone) describd by Folk (1973).

Glauconitization

The glauconitization process has been studied by many authors. In their authoritative review, Odin and Matter (1981) conclude that glauconitic facies are generally developed in open marine, low energy and slightly reducing environments with low sedimentation rates and with temperatures in the range 7 to 15°C. Too warm and too oxidizing water destroys glauconitic minerals at depth of less than 30 m. However, the green pellets may occur at water depth of more than 350 m.

The similarity in form between the glauconite grains in the studied microfacies and the overlying algal pellets may suggest that they were originally pellets of algal origin. The mechanism of the biological corrosion - chemical dissolution of carbonate by bacteria suggested by Golubic and Schneider (1979) may have applied to explain the chemical dissolution of the initial algal pellets. This mechanism could result in the creation of the semi-confined microenvironment proposed by Odin and Giresse (1972) and Odin and Matter (1981) as an essential factor in the glauconitization process. The bacterial activity could have caused both the regular dissolution of the carbonate in the original pellets and the regular slow exchanges of elements forming glauconite grains simultaneously.

Dolomitization

Dolomitization model for sucrosic dolostone has been described by Morrow (978, 1982). He suggested that it is formed as the result of grain growth from an

initial state where very finely crystalline dolomite euhedra are scattered throughout a limestone. The distributed dolomite crystals then progress towards a totally dolomitized fabric of sucrosic dolostone. Two stages of this model can be observed in the dolomitic biomicrite overlying the ferruginous pyrite-biomicrite (Fig. 5B ii) and in the mottled dolostone with sucrosic textures (Fig. 5B iv).

Geochemical analysis including a stable isotope measurements were carried out on 7 bulk samples of the mottled dolomite. From these analyses, Na^+ and Sr^{2+} concentrations provide an indication of the relative salinities of the environment during neomorphism (Randazzo *et al.* 1983). The sodium content of modern dolomites is generally more than 2000 ppm whereas most ancient dolomites have concentrations lower than 1000 ppm (Land and Hoops 1973, Mattes and Mountjoy 1980). However, strontium concentrations of modern dolomites average greater than 640 ppm (Behrens and Land 1972) while the majority of ancient dolomites are less than 350 ppm (Kinsman 1969, Mattes and Mountjoy 1980). The Na^+ concentration of the mottled dolomites in the present study ranges from 278 to 927 ppm, with an average of 560 ppm, whereas the Sr^+ concentration ranges from 185-232 ppm with an average of 200 ppm. The lower concentration of both Na^+ and Sr^{2+} indicate that the studied dolomite was formed from diluted saline water which resulted form mixing of fresh and normal saline waters. The mole % $Mg CO_3$ generally ranges from 24 to 27%. These low values are interpreted as the result of the recalcification process (dedolomitization) and are not related to the relative salinity of the environment of deposition.

Stable Isotope Data

The range of $\delta^{18}O$ for the studied dolomite is from -3.1 to -4.64‰ (PDB), with the mean value being -3.8. The most enriched sample -3.1‰ is coarse and more intensively calcitized (dedolomitized) than the depleted sample. Values of $\delta^{13}C$ ranges from $+1.4$ to $+1.2$‰ (PDB). The mean value being $+1.25$, which is typical of "normal marine" carbon (Keith and Weber 1964). Although the negative values of $\delta^{18}O$ could conceivably represent the effect of light meteoric water, they could equally represent (1) a universal biological effect in older carbonate; (2) higher temperature of precipitation; (3) an isotopically lighter ocean (Hudson 1977). The mean oxygen and carbon values (-3.8‰ and $+1.25$‰ PDB respectively) are similar to those of fresh water/saline water mixing (Dorage dolomite) as shown by Mattes and Mountjoy (1980).

Weathering

Oxidation of Pyrite

The exposure of the studied microfacies to oxygenated ground waters establishes the aerobic environmental conditions, essential for the iron transformation.

Singer and Stumm (1970) showed that under acidic conditions and in the absence of bacteria, Fe^{3+} was a much more effective catalyst of pyrite oxidation than was ferrous iron. However, they propose that in natural acidic environments and in the presence of iron oxidising bacteria, the rate of pyrite oxidation is higher. This is because the reduced iron (Fe^{2+}) is biologically oxidised to ferric iron (Fe^{3+}) which then oxidises the pyrite according to the nominal equation:

$$14\ Fe^{3+} + Fe\ S_2 + 8\ H_2O \longrightarrow 15\ Fe^{2+} + 2\ SO_4^{2-} + 16\ H^+$$

Although the details of the reactions are incompletely understood, their products are recognized in the presently studied microfacies in the form of gypsum which infills pore spaces and fractures, goethite and hematite (Fig. 6). The presence of gypsum may indicate that the released SO_4^{2-} anions have reacted with Ca^{2+} cations from ground water whereas the presence of goethite and hematite may suggest that the iron oxyhydroxides, principally goethite (Fe O OH) (Berner 1971, Turner 1980), was formed by oxidation and hydrolysis of the produced Fe^{2+}. The goethite was then dehydrated during diagenesis to hematite. The maximum temperature at which fine grained goethite is stable relative to hematite plus pore water is about 40°C (Berner 1969). On this basis, Turner (1980) assumed that fine grained goethite is unstable relative to hematite under virtually all geological conditions and that dehydration takes place in the presence of water.

Weathering of Glauconitic Facies

Several authors agree that water is the single most important agent in the chemical weathering of silicates (Degens 1965, Krauskopf 1967, Loughnan 1969, Berner 1971, Carroll 1970). Many other authors showed that the weathering process could proceed by the formation of metal-organic complexes by biogenic acids and other organic compounds (Tsyurupa 1964, Arrieta and Grez 1971, Berthelin *et al.* 1974; Tan 1975, Griffith and Schnitzer 1975; Peredue *et al.* 1976). Silverman (1979) reviewed and discussed the biogeochemical weathering of silicates and showed that the primary role is played by hydrogen ions produced either by dissolution of water molecule or by hydrolysis at the mineral water interface.

El Sharkawi and Khalil (1977) showed that the intensive weathering of glauconite leads to the formation of white alunite and low grade limonitic ore at El Gidida area, Bahariya Oases, Egypt. They postulated that the glauconitic cover shared in the development of the iron ore beds, by leaching and infiltration followed by subsequent deposition in the underlying "calcareous" rocks. In the present study the author suggests that the decomposition of the studied glauconitic sediments resulted in the formation of ferruginous ooids. The intensive weathering of the glauconite grains released Si, Mg, K, and Al and concentrated Fe. Some of the released silica has grown on the quartz grains. Other parts of the silica are

believed to be combined with Al to form kaolinite - goethite and then, as alteration proceeds, the kaolinite is altered to aluminous goethite and hematite (Parron *et al.* 1976). The Mg released could have participate in the dolomitization process. Because of the rapid oxidation of Fe^{2+} to Fe^{3+} and formation of ferric oxyhydroxide (mostly goethite) which dehydrated into hematite, the weathered zones in the glauconite grains are gradually pseudomorphed by the ferruginous matrix.

According to the different intensities of weathering in different zones, an orange coloured ferruginous matrix and red non-oriented ferruginous matrix were produced successively defining a concentrically layered envelope around the ferruginous ooids. This process is isovolumetric and occur with preservation of the original volume of the sediments involved (Bonifas 1959, Millot 1970). Some of the ooids which exhibit normal and superficial ooid types show such successive alternations of orange and red colour layers. The red colour layers are completely pseudomorphed by iron, whereas the orange layers show little concentration of silica and aluminium. However, the nuclei of those grains also show concentration of silica and aluminium. This may indicate the transitional stages from glauconite grains to ferruginous ooids and argue for the mechanism of formation of ferruginous ooids by weathering as has been reviewed and discussed by Parron and Nahon (1980) and Nahon *et al.* (1980).

Recalcification (Dedolomitization) Process

Under subaerial weathering conditions, circulating alkaline water can breakdown the ferrous iron of the dolomite and produce iron hydroxides (Al Hashimi and Hemingway 1973). The association of rhombic hematite with the partial or complete replacement of some rhombic ankerite by granular calcite indicate that the studied sucrosic mottled dolostone was subjected to subaerial weathering by ground water. The iron released from ankerite crystals has generally accumulated in the pore spaces or along the rhombic cleavages of the crystals, sometimes iron pseudomorphs the rhombs completely (Fig. 5B, iv). The pore spaces filled with iron oxide and giving the rock its mottled character are produced either through dissolution of pre-existing aragonite pore fillings or from shell fragments (Fig. 5B, i).

Paragenesis

From textural relationships and mineralogical composition identified using X-ray diffraction (Fig. 6) and SEM techniques, the paragenetic sequence for each microfacies are summerized in the following Table:

Syngenetic stage	Diagenetic stage		Surficial weathering
	Early	Late	
4- Deposition of quartzarenite	Formation of glauconite in pore spaces	Partial decomposition of glauconite grains	Intense decomposition of glauconite and dissolution of quartz grains
3- Deposition of biomicrite	Formation of scattered ankerite crystals	Formation of sucrosic dolostone	Formation of mottled dolostone
2- Deposition of sandy pelbiomicrite	Formation of glauconite grains	Partial decomposition of glauconite grains	Formation of ferruginous glauconitic ooids
1- Deposition of biomicrite	Formation of framboidal pyrite	Pereferential solution of some shell fragments	Formation of goethite, hematite and gypsum

Conclusion

Four prominent microfacies within the Coniacian - Santonian sediments of the Abu Zenima area display important post depositional chemical, mineralogical and textural changes in which ground water and bacteria have played the main role. The most significant changes are:

1) Formation of hematite, goethite and gypsum as the result of hydrolysis and oxidation of framboidal pyrite crystals disseminated in the recrystallised biomicrite.
2) Formation of ferruginous ooids as the result of weathering of the glauconitic sediments.
3) Formation of mottled dolostone due to the oxidation and recalcification of the sucrosic dolostone.
4) Weathering of the glauconitic quartzarenite resulting in the formation of Lepidocrocite, goethite and hematite and corrosion of the quartz grains.

Acknowledgement

The author is grateful to Prof. Dr. E.M. El Shazli and Prof. Dr. Z.M. Zaghloul for their useful discussions. He also expresses his gratitude to the Institute of Geology, University of Bergen, Norway, for assistance received in making the chemical analyses.

References

Al Hashimi, W.S. and **Hemingway, J.E.** (1973) Recent dedolomitization and the origin of the rusty crusts of North Umberland. *J. Sed. Petrol.* **43** 82-91.

Arrieta, L. and **Grez, R.** (1971) Solubilization of iron-containing minerals by soil microorganisms. *Appl. Microbiol.* **22:** 487-490.

Berner, R.A. (1969) The Synthesis of framboidal pyrite. *Econ. Geol.* **64:** 383-384.

Berner, R.A. (1971) *Principles of chemical sedimentology.* Internat. series in Earth and Planet-Science. McGraw-Hill, New York, 240 pp.

Behrens, E.W. and **Land, L.S.** (1972) Subtidal Holocene dolomite, Baffin Bay, Texas, *J. Sed. Petrol.* **42:** 155-161.

Bonifas, M. (1959) Contribution à l'étude géochimique de l'altération Lateritique: Strasbourg, *Mém. Serv. Carte Géol. Als. Lorr.* **17:** 159 p.

Berthelin, J., Kogblevi, A. and **Dommergues, Y.** (1974) Microbial weathering of a brown forest soil: influence of partial sterilization. *Soil Biol. Biochem.* **6:** 393-399.

Carroll, D. (1970) *Rock weathering.* Plenum, New York, 203 p.

Clark, G.R. and **Lutz, R.A.** (1980) Pyritization in the shells of living bivalves. *Geology*, **8:** 268-271.

Dahanayake, K. (1977) Classification of oncoids from the Upper Jurassic carbonates of the French Jura. *Sedimentary Geol.* **18:** 337-353.

Degens, E.T. (1965) *Geochemistry of sediments.* Prentice-Hall, Englewood Cliffs, NJ, 342 p.

El Sharkawi, M.A. and **Khalil, M.A.** (1977) Glauconite, a possible source of iron for El Gidida Iron Ore Deposits, Bahariya Oases, Egypt. *Egypt. J. Geol.* **21:** 109-116.

Folk, R.L. (1973) Carbonate petrography in the Post-Sorbian age *in:* **R.N. Ginsburg, (ed.),** *Evolving Concepts in Sedimentology*, The John Hopkins University studies in Geology, No. **21:** 118-158.

Folk, R.L. (1974) *Petrology of Sedimentary Rocks.* Austin, Texas Univ. Hemphill's Bookstore. 182 p.

Gebelein, C.D., Steinen, R.P., Garrett, P., Hoffman, E.J., Queen, J.M. and **Plummer, L.N.** (1980) Subsurface dolomitization beneath the tidal flats of central west Andros Island, Bahamas: *in:* **D.H. Zenger, J.B. Dunham** and **R.L. Ethington, (eds.),** *Concepts and models of dolomitization. Soc. Econ. Paleontol. Mineral. Spec. Publ.* **28:** 31-49.

Ghorab, M.A. (1961) Abnormal stratigraphic features in Ras Gharib oilfield: *3rd Arab Petrol. Cong.* Alexandria, Egypt. **11:** 10 p.

Goldhaber, M.B. and **Kaplan, I.R.** (1974) The sulfur cycle, *in:* **E.D. Goldberg (ed.),** *The sea*, vol. **5:** *Marine chemistry*, J. Wiley interscience, London pp. 569-655.

Golubic, S. and **Schneider, J.** (1979) Carbonate dissolution, *In:* **Trudinger, P.A.** and **Swaine, D.J. (eds.)** *studies in environmental science* 3, Biogeochemical cycling of mineral-forming elements, Elsevier, Amsterdam - Oxford - New York, pp. 107-129.

Griffith, S.M. and **Schnitzer, M.** (1975) The isolation and characterization of stable metal organic complexes from tropical volcanic soils. *Soil sci.* **120:** 126-131.

Grossman, R.H., Lebling, R.S. and **Scherp, H.S.** (1979) Chlorite and its relationship to pyritization in anoxic marine environments. *J. Sed. Petrol.* **49:** 611-614.

Howarth, R.W. (1979) Pyrite: its rapid formation in a salt marsh and its importance in ecosystem metabolism. *Science* **203:** 49-51.

Hudson, J.D. (1977) Stable isotopes and Limestone Lithification, *J. Geol. Soc.* London **133:** 637-660.

Keith, M.L., and **Weber, J.N.** (1964) Isotopic composition and environmental classification of selected limestone and fossils. *Geochim. Cosmochim. Acta* **28:** 1787-1816.

Kinsman, D.J.J. (1969) Interpretation of Sr^{2+} concentrations in carbonate minerals and rocks. *J. Sed. Petrol.* **39:** 486-508.

Krauskopf, K.B. (1967) *Introduction to geochemistry.* McGraw-Hill, New York, 721 p.

Krouse, H.R. and **McCready, R.G.L.** (1979) Biogeochemical cycling of sulfur, *In:* **Trudinger, P.A.** and **Swaine, D.J. (eds.),** *Studies in Environmental Science* 3, Biogeochemical cycling of mineral-forming elements, Elsevier, Amsterdam, Oxford, New York, pp. 401-430.

Land, L.S. and **Hoops, G.K.** (1973) Sodium in carbonate sediments and rocks: a possible index to the salinity of diagenetic solutions. *J. Sed. Petrol.* **43:** 614-617.

Loughnan, F.C. (1969) *Chemical weathering of the silicate minerals.* Elsevier, New York, 154 p.

Mattes, B.W. and **Mountjoy, E.W.** (1980) Burial dolomitization of the Upper Devonian Miette Buildup, Jasper National Park, Alberta. *In:* **Zenger, D.H., Dunham, J.B.** and **Ethington, R.L. (eds.),** *concepts and models of dolomitization, Soc. Econ. Paleontol. Mineral, Spec. Publ.* **28:** 259-297.

Millot, G. (1970) Geology of clays: *Weathering Sedimentology, Geochemistry*, Farrand, W.R., and Paquet, H., (trans.): New York, Springer - Verlag, 425 p.

Morrow, D.W. (1978) The influence of the Mg/Ca ratio and salinity on dolomitization in evaporite basins: *Canadian Soc. Petrol. Geol. Bull.* **26:** 389-392.

Morrow, D.W. (1982) Diagenesis 2. Dolomite - part 2. Dolomitization models and ancient dolostones: *Geo-science* Canada, **9:** 95-107.

Nahon, D., Carozzi, A.V. and **Parron, C.** (1980) Lateritic weathering as a mechanism for the generation of ferruginous ooids. *J. Sed. Petrol.* **50:** 1287-1298.

Odin, G.S. (1975) *De glauconiarum, Constitution, Origine, Aetateque. Recherches sédimentologiques et géochimiques sur La gènese des glauconies actuelles et anciennes; application à la révision de l'échelle chronostratigraphique:* Thèse d'Etat, Univ. de Paris, 280 p.

Odin, G.S. and **Giresse, P.** (1972) Formation de minéraux phylliteux (berthiérine, smectites ferrifères, glauconite ouverte) dans les sédiments du Golfe du Guinée. *C.R. Acad. Sc. Paris,* **275:** 177-180.

Odin, G.S. and **Matter, A.** (1981) De glauconiarum origine. *Sedimentology,* **28:** 611-641.

Parron, C., Nahon, D., Fritz, B., Paquet, H. and **Millot, G.** (1976) Desilicification et quartzification par alteration des grès albiens du Gard. Modeles géochimiques de la gènese des dalles quartzitiques et silcretes. *Bull. Sci. Geol.* **29:** 273-284.

Parron, C. and **Nahon, D.** (1980) Red bed genesis by lateritic weathering of glauconitic sediments. *J. Geol. Soc. London,* **137:** 689-693.

Perdue, E.M., Beck, K.C. and **Reuter, J.H.** (1976) Organic complexes of iron and aluminium in natural waters. *Nature* **260:** 418-420.

Randazzo, A.F., Sarver, T.J. and **Metrin, D.B.** (1983) Selected geochemical factors influencing diagenesis of Eocene carbonate rocks, peninsular Florida, U.S.A., *Sedimentary Geol.* **36:** 1-14.

Siever, R., and **Kastner, M.** (1972) Shale petrology by electron microprobe, pyrite - chlorite relations, *J. Sed. petrol.* **42:** 350-355.

Silverman, M.P. (1979) Biological and Organic chemical decomposition of silicates, *In:* **Trudinger, P.A.** and **Swaine, D.J. (eds.)** *studies in Environmental Science 3,* Biogeochemical cycling of mineral-forming elements, Elsevier, Amsterdam - Oxford - New York, pp. 445-465.

Singer, P.C. and **Stumm, W.** (1970) Acid mine drainage: The rate limiting step. *Science* **167:** 1121-1124.

Sweeney, R.E. and **Kaplan, I.R.** (1973) Pyrite framboid formation: Laboratory synthesis and marine sediments. *Econ. Geol.* **68:** 618-634.

Tan, K.H. (1975) The catalytic decomposition of clay minerals by complex reaction with humic and fluvic acid. *Soil. Sci.* **120:** 188-194.

Tsyurupa, I.G. (1964) Some data on complex products of microbial activity and autolysis with soil minerals. Sov., *Soil. Sci.* No. **3:** 261-265.

Turner, P. (1980) Continental Red beds, Development in Sedimentology 29, Elsevier Scientific Publishing Co., Amsterdam - Oxford - New York, 562 p.

Wolf, K.H. (1965) Petrogenesis and Paleoenvironment of Devonian algal limestones of New South wales. *Sedimentology* **4:** 113-178.

(Received 25/11/1984;
in revised form 01/04/1985)

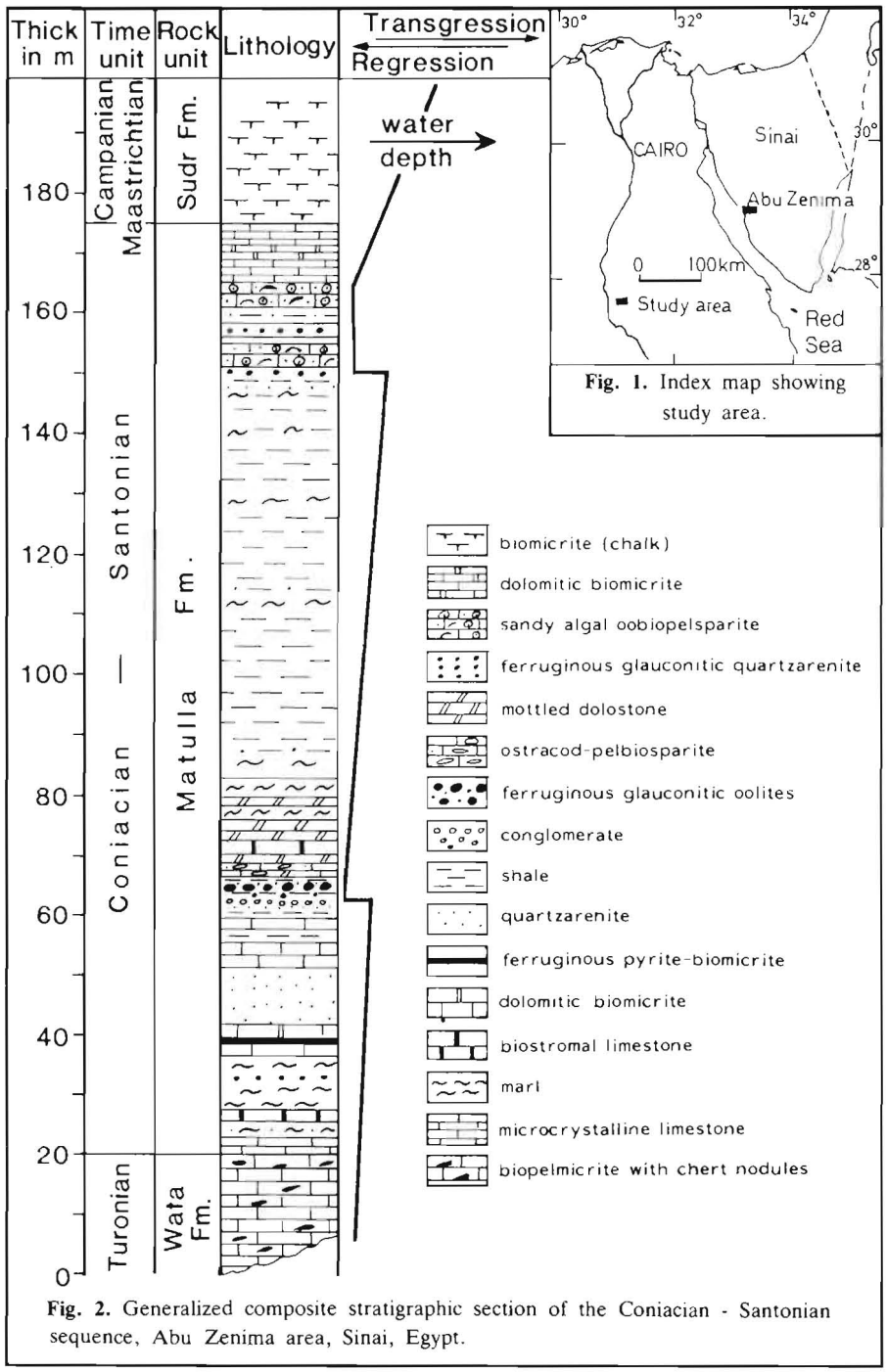

Fig. 1. Index map showing study area.

Fig. 2. Generalized composite stratigraphic section of the Coniacian - Santonian sequence, Abu Zenima area, Sinai, Egypt.

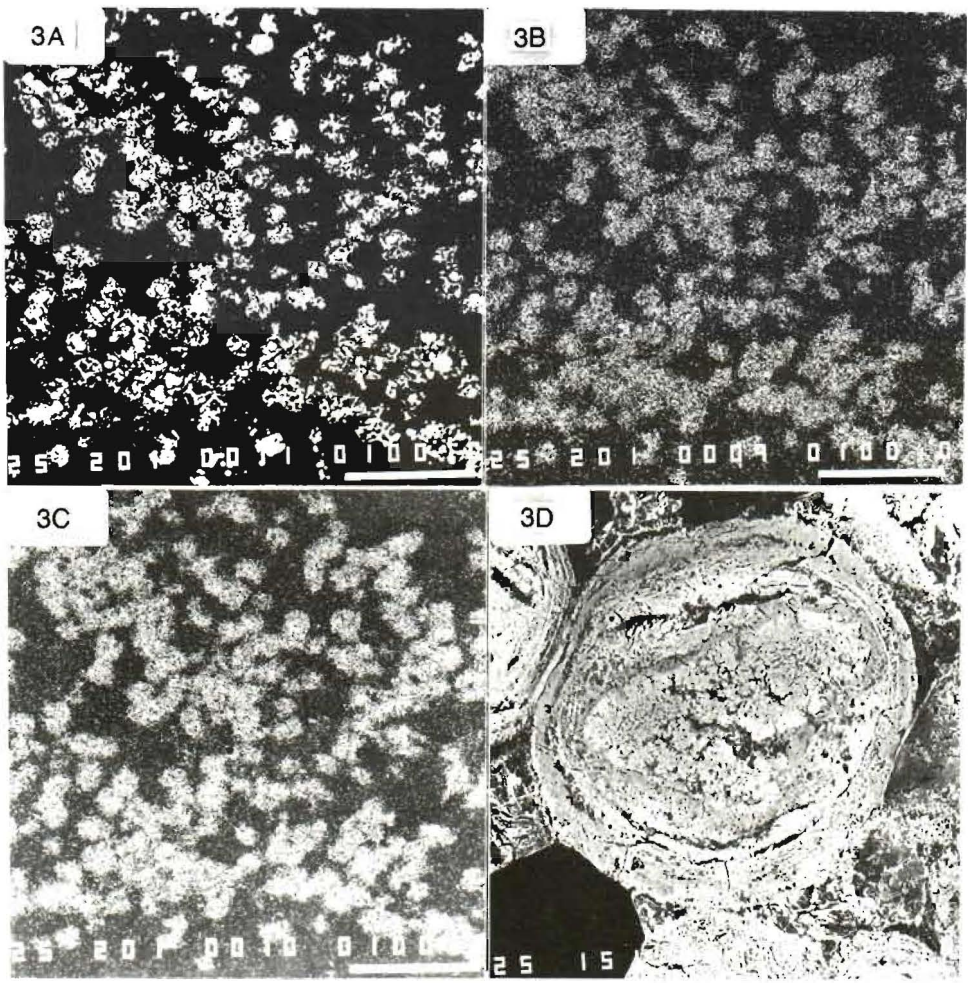

Fig. 3-A. Back scattered electron micrograph of framboidal iron sulphide crystals.

Fig. 3-B and C. X-ray mapping of iron and sulphur respectively in the framboidal iron sulphide crystals.

Fig. 3-D. Back scattered electron micrograph of ferruginous ooid grain showing that the concentric layers are produced by weathering of glauconite grain.

Scale Bar = 100 μm.

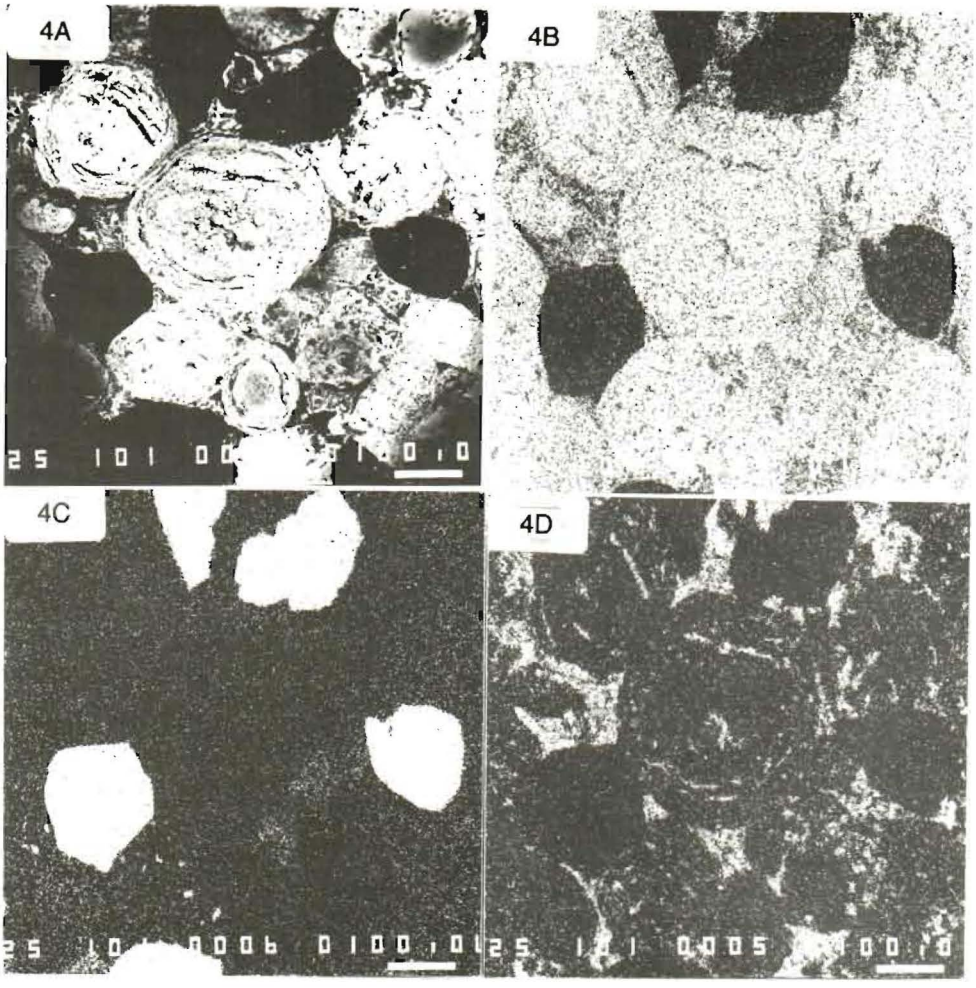

Fig. 4-A. Back scattered electron micrograph of sandy ferruginous oolites.

Fig. 4-B, C and D. X-ray mapping of iron, silica and calcium respectively. Photographs illustrated that the ooids are formed mainly of iron with traces of silica. High concentration of silica in the small ferruginous ooid indicates the different intensities of weathering in the studied rock unit. Calcium is mainly concentrated in fractures.

Scale Bar = 100 μm.

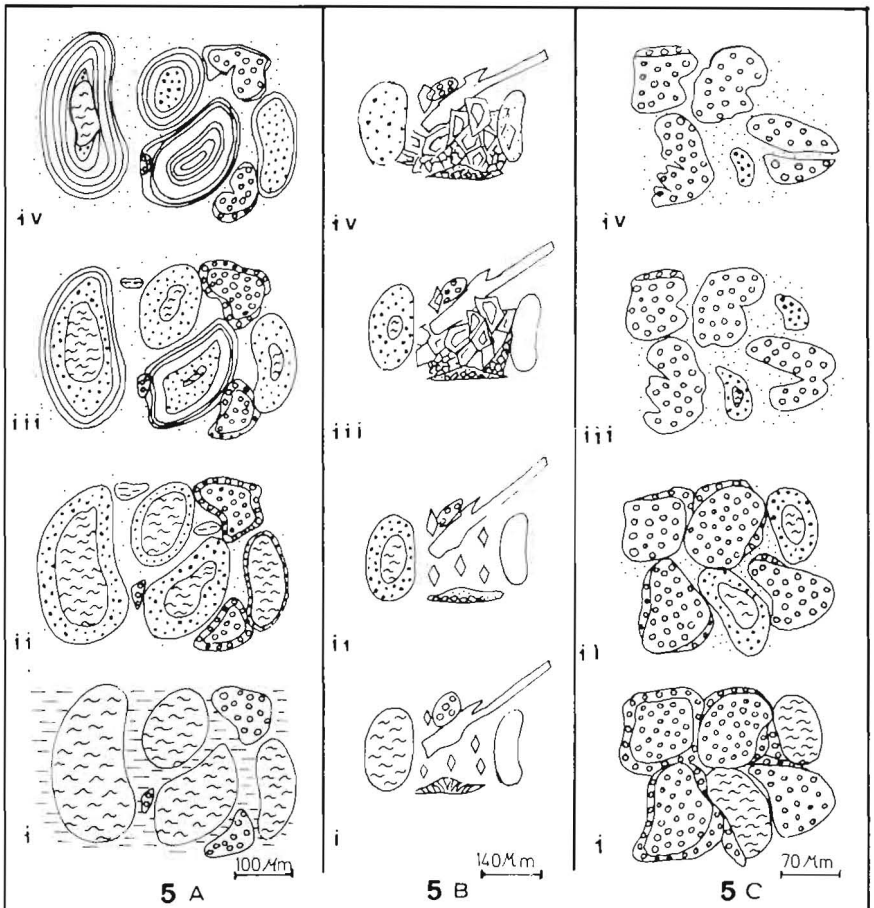

Fig. 5-A. Petrographic evolution of sandy glauconitic facies.

Fig. 5-B. Petrographic evolution of mottled dolostone.

Fig. 5-C. Petrographic evolution of glauconitic quartzarenite.

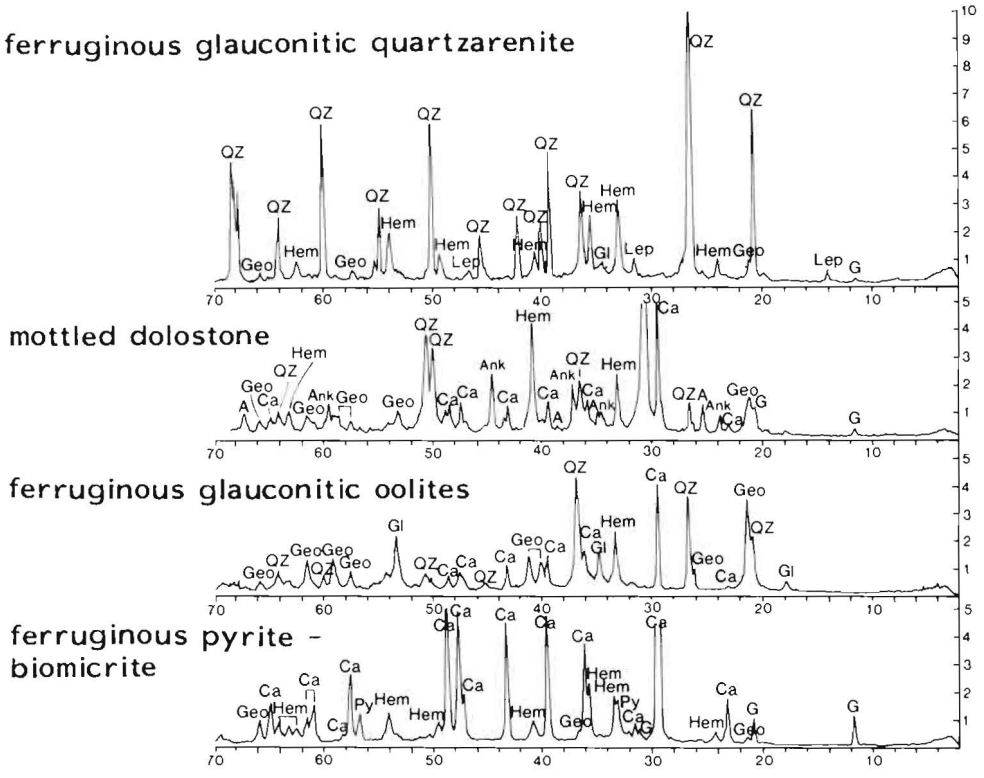

Fig. 6. X-ray diffraction pattern of representative powdered bulk samples from Coniacian - Santonian ferruginous sediments at Abu Zenima area, Sinai, Egypt.

أصل أكاسيد الحديد والبطروخ الحديدي في صخور عصري الكونياس والسانتوني بمنطقة أبو زنيمة ـ سيناء ـ مصر

السيد عبد العزيز علي يوسف

كلية العلوم ـ جامعة القاهرة ـ القاهرة ـ مصر

يهدف هذا البحث إلى توضيح أصل أكاسيد الحديد والحجر الحديدي البطروخي المميزة لصخور عصري الكونياس والسانتوني بمنطقة أبو زنيمة بوسط غرب سيناء. يرتبط وجود هذه الأكاسيد والحجر الحديدي البطروخي بأربع سحنات تتميز بتغيرات معدنية وكيميائية ونسيجية أساسية حدثت بعد الترسيب. يعزى الباحث هذه التغيرات إلى نشاط البكتريا وعمليات التجوية.

تتمثل السحنات موضع الدراسة بطبقات رقيقة من الحجر الجيري العضوي الغني بحبيبات البيريت، الحجر البطروخي الجلوكونيتي، الحجر الدولوميت المبقع والحجر الرملي الجلوكونيتي. تكون البطروخ الحديدي في مكانه نتيجة لعمليات التجوية لحبيبات الجلوكنيت في حين تكونت البقع المميزة لصخور الدولوميت نتيجة لأكسدة وكلسنة الدولوميت (الانكيريت) وحبيبات الجلوكونيت وتجميع هذه الأكاسيد في الفجوات الموجودة في الصخر.

تتكون المواد الحديدية الموجودة في هذه الصخور موضع الدراسة من أكاسيد الهيماتيت والجوتيت والليبيدوكروسيت.